9

Magnetic properties of transition metal complexes

9.1 Introduction

In the last chapter, in Section 8.4, it was suggested that the spin of an electron is best thought of as meaning that the electron behaves like a tiny bar magnet. When there are several unpaired electrons the spin degeneracies can be thought of as resulting from the variety of ways of arranging bar magnets side-by-side. Similarly, the orbital motion of the electron, the circulation of charge around the nucleus, can be thought of as leading to a solenoid-like magnet. These spin and orbital magnets will interact with an applied magnetic field, so that when an atom or molecule is placed in a magnetic field any spin degeneracy may be removed—the different resultant magnets behave differently. Thus, a level which is orbitally non-degenerate but is a spin doublet has this spin degeneracy split into two levels with slightly different energies in a magnetic field (corresponding to the N–S and S–N arrangements). If there is orbital degeneracy this too may be removed by a magnetic field. As we shall see, it is such splittings which determine the magnetic properties of a complex. Note particularly that either or both of spin and orbital degeneracies give rise to the magnetic effects. Sometimes statements such as 'the number of unpaired electrons in a complex may be determined from magnetic susceptibility measurements' are encountered. Whilst true within their own context, they should not be read as meaning that in electron spin lies the sole source of magnetic effects.

The splittings produced by magnetic fields are very small, about 1 cm^{-1} for a field of 0.5 T, and, for the majority of cases, are proportional to the magnetic field. Because the splittings are so small, any particular atom or molecule may be in any one of the several closely spaced states resulting from the splitting. For a macroscopic sample, however, there will be a Boltzmann distribution between the levels; at room temperature kT is about 200 cm^{-1} so ample energy is available. Clearly if we are to be able to interpret

S. F. A. Kettle, *Physical Inorganic Chemistry*

experimental results, we must consider both the splittings and the Boltzmann distribution over them. However, because the effect of the magnetic field is so small we must consider any other interaction which involves energies corresponding to more than about 1 cm^{-1}. This is because such interactions will play a part in determining the ground state of the complex before the magnetic field is switched on—this field will only cause the subsequent splitting. Two such interactions—spin–orbit coupling and the presence of low-symmetry components in what is otherwise an octahedral crystal field—have already been discussed in outline. The latter effect can seldom be neglected. One might think, for example, that an isolated $[Co(NH_3)_6]^{3+}$ ion would be accurately octahedral. This is not so, for there is an incompatibility between the threefold axis of each NH_3 and the coincident fourfold axis of the CoN_6 octahedron. Add to this the effect of the environment (and this means 'do not consider an isolated molecule; in solution it will be surrounded by a jumble of solvent molecules and in a crystal by anions—and these will seldom respect its octahedral symmetry'), recall the Jahn–Teller effect, remember that some metal–ligand vibrations will be thermally excited down to quite low temperatures and that lattice vibrations will persist to an even lower temperature, and it becomes evident that from the point of view of magnetism, a regular octahedral environment is a rare, if not extinct, species. For basically octahedral molecules, however, an octahedral model is a good first approximation and may be refined to take account of the above effects. For the majority of this chapter we shall confine ourselves largely to such octahedral complexes.

Before we can proceed, some of the vocabulary of magnetism has to be introduced. Closed shells of electrons have neither spin nor orbital degeneracy and are represented by a single wavefunction. A magnetic field therefore produces no splitting. It does, however, distort the electron density slightly, in a manner akin to that predicted by Lenz's law in classical electrodynamics. That is, effectively, a small circulating current is produced, the magnetic effect of which opposes the applied magnetic field. Because there is no resistive damping, the current remains until the magnetic field is removed. Molecules with closed shells are therefore repelled by a magnetic field and are said to exhibit diamagnetism or to be *diamagnetic*.

Suitably oriented magnets are attracted towards the magnetic field of a stronger magnet and the same is true for any orbital magnet and the intrinsic (spin) magnet associated with an unpaired electron. Molecules with unpaired electrons are therefore attracted into a magnetic field[1] and are said to to exhibit paramagnetism or to be *paramagnetic*. For any transition metal ion which has both closed shells and unpaired electrons the diamagnetism of the former and the paramagnetism of the latter are opposed. All that can be measured is their resultant. Fortunately, the effect of paramagnetism is about 100 times as great as that of diamagnetism so that it takes a great deal of the latter to swamp the former. Fortunately, too, it is found that the effects of diamagnetism are approximately additive—each atom makes a known, and approximately constant, contribution to the diamagnetism of a molecule and so diamagnetism may be fairly accurately allowed for once the empirical formula of a complex is known. This means that it is possible to deduce the

[1] Exceptions to this statement exist at very low temperatures.

intrinsic paramagnetism of a complex to an acceptable level of precision and to compare it with theoretical predictions. Finally, a discussion in terms of an isolated molecule requires that the (para)magnetic units do not interact; that is, these units must be spatially well separated. The jargon is to say that the sample must be magnetically dilute. The detailed theory of magnetically non-dilute substances is beyond the scope of this book, although some general comments on the topic are contained in Section 9.12. Actually, measurements at very low temperatures have shown that some of the most classic of coordination compounds exhibit a tiny amount of magnetic coupling between the transition metal ions and so are slightly non-dilute. Examples include $K_3[Fe(CN)_6]$, $[Ni(en)_3](NO_3)_2$, $K_2[Cu(H_2O)_6](SO_4)_2$ and $[Ni(H_2O)_6]Cl_2$. At temperatures much above those of liquid helium such compounds behave as magnetically dilute.

9.2 Classical magnetism

A theory of magnetism was developed long before the advent of quantum mechanics. This section contains an outline of this theory and defines some of the experimental quantities which may well be encountered.

When a substance is placed in a magnetic field, H, the total magnetic induction within the substance, B, is proportional to the sum of H and M, where M is the magnetization of the substance:

$$B = \mu_0(H + M)$$

where μ_0 is the vacuum permeability (in the CGS system of units μ_0 is unity, in SI it is defined to be exactly $4\pi \times 10^{-7}\,\mathrm{N\,A^{-2}}$; note that $\mathrm{N\,A^{-2}}$ is the same as $\mathrm{H\,m^{-1}}$—either may be encountered). This equation may be written as

$$\frac{B}{H} = \mu_0\left(1 + \frac{M}{H}\right) = \mu_0(1 + \kappa)$$

where κ is the volume susceptibility (the ratio of the induced magnetization to the applied magnetic field). A more useful quantity is the susceptibility per gram, χ (chi), called the specific susceptibility, which is given by

$$\chi \times \frac{\kappa}{\rho}$$

where ρ is the density of the substance. Alternative forms of χ which are encountered are χ_A and χ_M, the atomic and molar susceptibilities, respectively. These latter are obtained by multiplying χ by the atomic and molecular weights, respectively, of the magnetically active atom or molecule. They are the susceptibilities per (gram) atom and mole, respectively. The former is no longer used but will be met in the older literature. Because our interest is in paramagnetism, some correction has to be made for the underlying diamagnetism, a topic dealt with in more length in Appendix 9. If such a correction has been made, it is indicated by a prime, thus χ'_A and χ'_M. Now,

$$\chi_M = \frac{\kappa}{\rho} \times (\mathrm{MW}) \times \frac{MV}{H}$$

where (MW) is the molecular weight and V is the molar volume. Therefore,

$$\chi_M = \frac{\text{total magnetization per mole}}{H}$$

$$= \frac{\text{average magnetization per mole} \times N_A}{H}$$

that is

$$\chi_M = \frac{\overline{m} N_A}{H} \tag{9.1}$$

where $\overline{m}$ is the average moment per molecule and N_A is Avogadro's number.

If we have a collection of identical molecules, each of magnetic moment μ and free to orient itself in a magnetic field, then in such a field there will be some alignment but this will be opposed by the thermal motion of the molecules. That is, the measured moment decreases with increasing temperature although μ itself is a constant. Langevin showed that in this situation the average (measured) magnetic moment $\overline{m}$, and the actual moment μ, are related by:

$$\overline{m} = \frac{\mu^2 H}{3kT} \tag{9.2}$$

a derivation of which will be found in almost every text on magnetism. His derivation contains the assumption that $B = \mu_0 H$, so the theory can only be expected to hold for gaseous molecules, although, as is commonly done, we shall ignore this limitation. Combining the last two equations we have

$$\chi_M = \frac{N_A \mu^2}{3kT} = \frac{N_A^2 \mu^2}{3RT} \equiv \frac{C}{T} \tag{9.3}$$

where C, the Curie constant, is equal to $N_A^2 \mu^2 / 3R$. The equation $\chi = C/T$ is known as the Curie law—susceptibility is inversely proportional to the absolute temperature. Surprisingly, this law is obeyed rather well by many liquids and solids, and in particular by complexes of the first row transition elements. The origin of this general agreement is not clear, except under rather special limiting conditions. The detailed quantum mechanical treatment does not at all readily lead to a prediction of a C/T type of behaviour. For complexes of the first row transition elements it turns out that the agreement is because the spin–orbit coupling constants are comparable in magnitude to kT; at low temperatures they do not follow the Curie law so well. Rearranging the above equation we find:

$$\mu = \frac{(3RT\chi_M)^{1/2}}{N_A} \tag{9.4}$$

It is convenient to express μ in units of Bohr magnetons,[2] β, and so we write $\mu = \mu_{\text{eff}}\beta$. Combining the last two equations we find that

$$\mu_{\text{eff}} = \frac{(3RT\chi_{\text{M}})^{1/2}}{N_{\text{A}}\beta} \tag{9.5}$$

Notice that, defined in this way, μ_{eff} is a pure number, the Bohr magneton number, which refers to a single molecule. Although often met, it is not strictly correct to call it the effective magnetic moment, and it certainly is incorrect to express it in units of Bohr magnetons, although this is a usage met all too often.

9.3 Orbital contribution to a magnetic moment

We now turn to the quantum mechanical approach to the phenomenon of paramagnetism and discuss first the orbital contribution to a magnetic moment. It is convenient at this point to make a few general statements which will be explained by the subsequent discussion.

The phrase orbital degeneracy was used in Section 9.1, implying that for individual cases one may or may not exist. If in the free ion—in the absence of a magnetic field—there is orbital degeneracy (that is, if we have anything other than an *S* state ion) the free ion has an *orbital magnet*. If the orbital degeneracy is lost in a real environment—by chemical bonding or crystal field effects—the orbital contribution to the total magnetic moment is said to be *quenched*. If the orbital degeneracy is merely reduced, the orbital contribution is partially or incompletely quenched. Orbital degeneracy, however, although a necessary condition for an orbital moment, is not a sufficient condition.

It may be recalled that in Section 8.4 the orbital moment was likened to the magnetic effect produced by a current in a solenoid. An even better analogy would be with the magnetic moment associated with a current flowing around a circular ring of superconducting material. If the superconducting ring is rotated by 90°—or any other angle—about its unique axis, one is left with a physically identical situation (for a solenoid the ends of the wire coil would be in a different position after the rotation). The requirement for a non-zero orbital-derived moment is similar. An orbital

[2] The Bohr magneton is a fundamental quantity in the quantum theory of magnetism. Bohr's explanation of atomic structure was based on the assumption that the angular momentum of an electron circulating about the nucleus of an atom is quantized and equal to $nh/2\pi$, where n is an integer and h is Planck's constant. That is, $nh/2\pi = ma^2\omega$, where m is the mass of the electron, a the radius of its orbit and ω its angular velocity in radians. The area of the circular orbit is πa^2 and the current to which the electron circulation is equivalent is $e \times (\omega/2\pi)$. From the theory of a current flowing through a circular loop of wire, the magnetic moment associated with the circulating electron is equal to the product

$$\text{current} \times \text{area} = \frac{e\omega}{2\pi} \times \pi a^2 = \frac{ea^2\omega}{2}$$

From Bohr's postulate, this equals

$$\frac{ea^2}{2} \times \frac{nh}{2\pi ma^2} = n\frac{he}{4\pi m} = n\beta, \quad \text{where } \beta = \frac{he}{4\pi m}$$

That is, the magnetic moment is an integer times β, where β is the Bohr magneton. It transpires that β is also the fundamental quantity in the modern quantum mechanical treatment.

degeneracy is needed—and this only occurs when orbitals are unequally occupied—but this orbital degeneracy must be such that there exist two or more degenerate orbitals which can be interconverted by rotation about a suitable axis. Consider the d_{zx} and d_{yz} orbitals in an octahedral complex, shown in Fig. 9.1. Rotation by 90° about the z axis interconverts these two orbitals, so that if an electron were initially in the d_{zx} orbital it could circulate about the z axis by jumping between the d_{zx} and d_{yz} orbitals alternately. This circulation is equivalent to a current flowing and so it produces a magnetic effect. The circulation may take place in either direction, clockwise or anticlockwise, and in the absence of a magnetic field the two possibilities are degenerate (this is implicit in the orbital degeneracy). On application of a magnetic field the two directions of circulation have different energies, and this is associated with the loss of orbital degeneracy in a magnetic field.

Four comments are relevant at this point. First, the d_{xy} and d_{zx} orbitals are interconverted by a rotation about the x axis and the d_{xy} and the d_{yz} by a rotation about the y axis, and so the discussion above is relevant to these pairs also. Second, a more detailed analysis shows that an electron in the d_{xy} orbital does not have to jump 90° to get into the d_{yz} orbital because these two orbitals overlap each other. Note that this statement is not incompatible with the fact that these two orbitals have a zero overlap *integral*. A continuous range of rotations is allowed, so that the electron cloud experiences no barrier to free rotation about the z axis. Third, the Jahn–Teller theorem requires that the orbital degeneracy which has just been invoked, actually, never exists! However, because they are largely non-bonding, it is usually assumed that any Jahn–Teller splitting of the d_{xy}, d_{yz} and d_{zx} degeneracy is small and that the orbital contribution to the moment is only slightly quenched. Physically, this means that an electron circulating about the z axis in the d_{zx} and d_{yz} orbitals does experience a barrier to free rotation but that this barrier is usually small relative to thermal energies. Finally, the d_{xy} and $d_{x^2-y^2}$ orbitals are interconverted by a 45° rotation about the z axis. However, in an octahedral complex they are not degenerate and so give rise to no magnetic effect. In a free atom, on the other hand, they *are* degenerate and so contribute to the orbital magnetic moment. Summarizing, it turns out that for octahedral transition metal ions, only ground states of T_{1g} and T_{2g} orbital symmetries give rise to orbital-derived magnetic moments. E_g ground states have no such moment.

A question which at once arises is 'can a complex which has no unpaired electrons be paramagnetic just because of its orbital magnetism'? The answer is yes; two examples are provided by the permanganate ion MnO_4^- and by the ion $[Co(NH_3)_6]^{3+}$. This seems strange. There is no case in which the ground state of a transition metal ion has orbital degeneracy without also having a spin degeneracy. So, both of the two examples just given have orbitally non-degenerate ground states and, of course, no spin degeneracy. We would expect them to be diamagnetic. Without orbital degeneracy, how can an orbital magnetism exist? The answer lies in the existence of an excited state in each case which *does* have the required orbital degeneracy and yet is a spin singlet. The magnetic field mixes some of the excited state into the ground state (or, equivalently, pushes a tiny bit of electron density into the excited state) and so the ground state assumes some of the properties of the excited. In particular, measurement shows that such a complex has

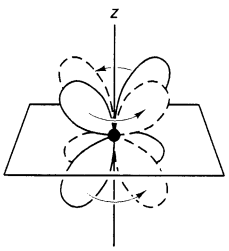

Fig. 9.1 The circulation of electron density about the z coordinate axis in an incompletely filled t_{2g} shell of an octahedrally coordinated transition metal ion. The electron density may be thought of as jumping from d_{zx} to d_{yz} to d_{zx} and so on, but see the text for a more accurate description.

a—small—orbital paramagnetism, which is sometimes large enough to cancel out the inherent diamagnetism. Because this paramagnetism does not depend on the thermal population of levels—unlike simple paramagnetism—it is called temperature independent paramagnetism, or TIP for short.[3] TIP is no mere academic curiosity. For diamagnetic transition metal ions it can be very important in determining the position of NMR resonances (the Co^{III} case is particularly well studied and is cited in the 'Further reading' at the end of Chapter 12). In Co^{II} octahedral complexes the magnitude of the TIP is often very comparable to the correction that has to be made for the underlying diamagnetism. In such cases, it is better to make no correction, and rely on the approximate cancellation of the two effects, than to correct for one but not the other.

9.4 Spin contribution to a magnetic moment

As has been mentioned earlier in this chapter, the phenomenon of electron spin is best thought of as the electron behaving like a tiny bar magnet. This bar magnet is essentially insensitive to its environment because the latter imposes an electrical, rather than a magnetic, field. A single bar magnet can be thought of as having two orientations with respect to an applied magnetic field, parallel and antiparallel, and these have different energies; with a pair of bar magnets the possibilities increase to three (both parallel, one parallel one antiparallel, both antiparallel), again each of the three arrangements have different energies. Higher spin multiplicities can similarly be given simple physical descriptions. It is possible to derive a simple equation which holds when the spin is the sole cause of the magnetic properties of a complex, and this will be done in Section 9.10. Despite its simplicity, we cannot immediately move to it because it is important to be aware of the circumstances in which it is applicable. These are when other, complicating, effects are absent. First, these complications must be explored. In the general case, both orbital and spin motions will contribute to the magnetism displayed by a complex; their effects may be additive or opposed. Further, the spin and orbital magnets may interact with each other, the phenomenon of spin–orbit coupling. This will be covered in the next section.

9.5 Spin–orbit coupling

Spin–orbit coupling has to be included in a discussion of the magnetic properties of transition metal complexes whenever a spin-derived magnetic moment and an orbitally-derived magnetic moment coexist. Spin–orbit

[3] It is instructive to look at the Co^{III} case in more detail. The d electron configuration of Co^{III} is $t_{2g}^6 e_g^0$ and so the ground state is $^1A_{1g}$. Earlier in the section it was found helpful to talk in terms of the magnetic properties of a current flowing in a ring of superconducting material. This analogy is helpful in the present context. In the point group O_h the set of three rotations R_x, R_y and R_z transform as T_{1g}. The analogy suggests that the components of the magnetic field also transform as T_{1g}. This is, indeed, the case. Now, if an excited state—call its symmetry species Γ—is to be mixed with the ground state, $^1A_{1g}$, by the magnetic field, then the direct product $T_{1g} \times \Gamma$ must contain $^1A_{1g}$, the symmetry of the ground state. This only occurs when $\Gamma = T_{1g}$ and so it has to be an excited $^1T_{1g}$ state that gives rise to the TIP of Co^{III} species. Reference to the d^6 Tanabe–Sugano diagram shows that such a low-lying excited state does, indeed, exist.

coupling splits terms with both spin and orbital degeneracy into a number of sublevels. This phenomenon is relevant to the spectroscopic properties of transition metal complexes and so in Table 8.2 were listed the number of components obtained as a result of spin–orbit coupling.

There is a simple method by which one may discover whether spin–orbit coupling mixes two d orbitals. For each d orbital, note the number of its nodal planes which also contain the z axis (i.e.those in which the z axis lies on a nodal plane). If two d orbitals differ by either one or zero in these numbers then the two orbitals may be mixed by spin–orbit coupling. Using this approach it follows that spin–orbit coupling mixes d orbitals as indicated below. Numbers in brackets indicate the number of nodal planes which, for that orbital, contain the z axis:

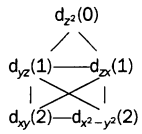

The origin of this pattern will become more evident from the detailed discussion that will be given Sections 11.4 and 11.5.

The magnitude of the spin–orbit coupling for a particular ion is usually given in terms of one of two different so-called spin–orbit coupling constants, ζ (zeta) and λ. The former is the one-electron spin–orbit coupling constant and is useful when comparing the relative magnitudes of spin–orbit coupling for different ions. In practice, for many-electron ions, what is measured is a resultant spin–orbit coupling between the resultant spin magnetic moment and the resultant orbital moment. It is this latter spin–orbit coupling constant which is called λ. For ground states the two constants are simply related:

$$\lambda = \pm\frac{\zeta}{2S}$$

where S is the spin multiplicity of the ion and the plus sign refers to d^1–d^4 ions and the minus sign to d^6–d^9. For these latter, it is simplest to think of holes circulating, the holes having the opposite charge to electrons. This point is detailed in appendix 12, which contains a specific example, although this particular appendix is specifically addressed to a problem that will be encountered in Chapter 11. Values for λ (and thence ζ) are obtained for free ions from atomic spectral data and for complex ions from magnetic measurements of the type discussed in this chapter.

9.6 Low-symmetry ligand fields

Because they can, and usually do, remove orbital degeneracies—and thus reduce the orbital contribution to the magnetism—low-symmetry ligand fields cannot be ignored in a study of the magnetic properties of transition metal complexes. Unfortunately, it is no easy matter to determine the splitting effects of low symmetry fields; usually it is necessary to work with two

splitting parameters. Because the effects of low symmetry are so much more important in magnetism than in, say, spectroscopy, the magnitude of the parameters is best determined magnetically. However, the values of the distortions may be small and so impossible to detect by any other method; the distortion may not even be evident in a structure determination, for instance. In this situation the magnitude of the parameter becomes something of a 'fudge factor'—it is given the value that produces best agreement between experiment and theory.

There is an important theorem due to Kramer, which states that when the ground-state configuration has an odd number of unpaired electrons there exists a degeneracy which a low symmetry ligand field cannot remove. This degeneracy, usually known as Kramer's degeneracy, arises from the fact that an orbital may be occupied by an electron in two ways—the spin may be up or it may be down. In the absence of a magnetic field these two orientations have the same energy. The application of a magnetic field causes the two to differ in energy—by about $1\,cm^{-1}$—and it is the greater occupation of the more stable in a macroscopic sample which causes the sample to be attracted into a magnetic field. When there is an even number of unpaired electrons a low-symmetry ligand field *can* relieve degeneracies, but the application of a magnetic field then causes the lowest state to become even more stable.

9.7 Experimental results

If there were no orbital contribution to the magnetic moment of a complex ion, one would have to worry a great deal less about the effects of spin–orbit coupling and low-symmetry fields. Table 9.1 lists the moments that would be expected for ions of the first transition series if there were no orbital contribution (spin-only moments) and compares these with room temperature experimental data. Also indicated in Table 9.1 is whether a significant orbital contribution is to be expected (that is, whether there is a ground state T_{1g} or T_{2g} term). In Section 9.10 the spin-only equation used to predict the moments given in Table 9.1 will be derived. On the whole, the agreement in this table is not at all bad and if all one is interested in is whether a complex is high or low spin then, if the oxidation state is known, a simple room temperature magnetic susceptibility measurement[4] on a tetrahedral or octahedral complex of a first-row element may readily be interpreted using the data in this table. A detailed analysis shows that the reasonable agreement between spin-only and experimental moments shown in Table 9.1 is somewhat fortuitous. For d^1–d^4 ions, spin–orbit coupling has the effect of reducing the observed moment and, roughly, cancels any orbital contribution. For d^6–d^9 ions, spin–orbit coupling increases the observed moment and adds to the orbital contribution. This, together with the increased magnitude of the spin–orbit coupling constants for these ions explains the few gross disagreements between spin-only and experimental values. Because of the very large spin–orbit coupling constants of elements of the second and third transition series, their complexes usually have moments much

[4] Appendix 8 contains both a description of how such measurements are made and the treatment of the data obtained; how the diamagnetic corrections are made, for instance.

Table 9.1 Comparison of calculated spin-only moments and experimental data for magnetic moments of ions of the first transition series

Ion	Configuration[a]	Orbital contribution expected?	Theoetical spin-only value	Range of experimental values found at room temperature
Octahedral complexes				
Ti^{3+}	d^1	Yes	1.73	1.6–1.75
V^{4+}	d^1	Yes	1.73	1.7–1.8
V^{3+}	d^2	Yes	2.83	2.7–2.9
Cr^{4+}	d^2	Yes	2.83	ca. 2.8
V^{2+}	d^3	No	3.88	3.8–3.9
Cr^{3+}	d^3	No	3.88	3.7–3.9
Mn^{4+}	d^3	No	3.88	3.8–4.0
Cr^{2+}	d^4 hs	No	4.90	4.7–4.9
Cr^{2+}	d^4 ls	Yes	2.83	3.2–3.3
Mn^{3+}	d^4 hs	No	4.90	4.9–5.0
Mn^{3+}	d^4 ls	Yes	2.83	ca. 3.2
Mn^{2+}	d^5 hs	No	5.92	5.6–6.1
Mn^{2+}	d^5 ls	Yes	1.73	1.8–2.1
Fe^{3+}	d^5 hs	No	5.92	5.7–6.0
Fe^{3+}	d^5 ls	Yes	1.73	2.0–2.5
Fe^{2+}	d^6 hs	No	4.90	5.1–5.7
Co^{2+}	d^7 hs	Yes	3.88	4.3–5.2
Co^{2+}	d^7 ls	No	1.73	1.8
Ni^{3+}	d^7 ls	No	1.73	1.8–2.0
Ni^{2+}	d^8	No	2.83	2.8–3.5
Cu^{2+}	d^9	No	1.73	1.7–2.2
Tetrahedral complexes[b]				
Cr^{5+}	d^1	No	1.73	1.7–1.8
Mn^{6+}	d^1	No	1.73	1.7–1.8
Cr^{4+}	d^2	No	2.83	2.8
Mn^{5+}	d^2	No	2.83	2.6–2.8
Fe^{5+}	d^3 hs	Yes	3.88	3.6–3.7
unknown	d^4 hs	Yes	4.90	
Mn^{2+}	d^5 hs	No	5.92	5.9–6.2
Fe^{2+}	d^6 hs	No	4.90	5.3–5.5
Co^{2+}	d^7	No	3.88	4.2–4.8
Ni^{2+}	d^8	Yes	2.83	3.5–4.0

[a] hs = high spin, ls = low spin.
[b] Note that low-spin tetrahedral complexes are very rare—if any exist at all—and are not included in this table.

smaller than the spin-only values. We shall see why this is so in Section 9.9. Lest it be thought that the sole effect of spin–orbit coupling is that of making life more complicated, it should be mentioned that a large spin–orbit coupling tends to reduce the sensitivity of the magnetic moment to low-symmetry fields, leading to a more octahedral-like behaviour—provided that the complex is approximately octahedral to start with.

9.8 Orbital contribution reduction factor

So far in this chapter an essentially crystal field approach has been followed. How has it to be modified to take account of covalency? One way is to let the spin–orbit coupling constant vary, to become a parameter, rather than giving it its free-ion value. Because a molecular orbital differs from an atomic orbital, we would expect them to have different magnetic moments and also different spin–orbit coupling constants. So, the t_{2g} set of d orbitals can give rise to an orbital contribution. What happens when it contains a ligand component—which, in this case, has to be π? The arguments used to justify an orbital contribution from the metal orbitals apply equally to the ligand π orbitals—the appropriate ligand combinations can be interchanged by suitable rotations, although it is unlikely that they will overlap with each other in the same way. The real question, therefore, is whether there is any reason to expect the ligand contribution to the moment to be equivalent to that part of the metal contribution which it has replaced. There is no such reason and so we must allow for the difference somewhere within our model. The usual way is to multiply the orbital contribution, calculated for the free metal ion, by a parameter, choosing that value of the parameter which gives the best agreement with experiment. This parameter is usually denoted k and is called the orbital reduction factor because it generally turns out to have a value of less than unity.

9.9 An example

This Section gives an outline of an algebraic calculation of the magnetic properties of a complex ion. The treatment is repeated in more detail in Appendix 10. In real life, the calculations would be carried out by a computer and some of the approximations that will be made here would not be necessary. However, the language of the subject is so wedded to the algebraic treatment that it is essential to study it, at least superficially.

The problem that will be considered is very simple, at least in principle. It is that of an octahedral t_{2g}^1 complex. So, the theory is that of a strong field complex of Ti^{III}—strong field because the e_g orbitals are considered so high in energy that they can be ignored. It would be good at the end of our development to be able to say that the final equation gives an excellent account of the magnetic properties of Ti^{III} complexes. Unfortunately, it is not possible to be so enthusiastic—indeed, it is possible that the theory is fundamentally flawed, although it will only be possible to appreciate why this is so after the theory has itself been developed.

The t_{2g}^1 configuration gives rise to a $^2T_{2g}$ ground term—three orbital functions, each of which may be combined with either of two spin functions, giving a total of six functions to be considered. Eventually, we will arrive at a picture in which these six levels, although clustered together, are split apart. We will be concerned with the Boltzmann distribution over these separated levels and, in particular, the sensitivity of the distribution to the application of a magnetic field. In this situation, it would clearly be ridiculous to consider just the effects of the magnetic field and to ignore the larger effects of any distortion and of spin–orbit coupling. For simplicity, a distortion from octahedral which retains some orbital degeneracy will be considered. This

means a distortion which retains either a fourfold or a threefold axis. Both are mathematically similar, only one additional low-symmetry field splitting parameter being involved in either case. Of the two it is simpler to consider the tetragonal case because we can then retain the coordinate axes of the octahedron. Such a tetragonal distortion leads to the orbital triplet (t_{2g}) splitting into an orbital singlet (b_{2g}) and an orbital doublet (e_g), the latter two labels being appropriate to D_{4h} symmetry. We will assume that the doublet is the lower in energy. Formally, we have two wavefunctions, a $^2B_{2g}$ term, above a set of four wavefunctions, a ^2E_g. Spin–orbit coupling splits the ^2E_g into two doublets. The final pattern is one with three distinct levels, each doubly degenerate, each a Kramer's doublet. These double degeneracies can only be split by a magnetic field.

All that remains is to remove the Kramer's degeneracies by the application of a magnetic field. Here, there is a clear divergence between the computer and algebraic solutions to the problem. In the algebraic approach, a distinction is made between the effect of a magnetic field on a particular level itself (the so-called first-order Zeeman effect) and its effect in mixing different levels together (the second-order Zeeman effect). The first-order Zeeman effect is proportional to the magnetic field strength, H, and the second order to the square of the magnetic field. Computer calculations show that this separation into terms proportional to H and to H^2 is only approximate, although for the strength of magnetic fields that are used in experimental work, the approximation is usually a good one.

The pattern of splittings that has just been described is shown in Fig. 9.2, where it has been assumed that the tetragonal field and the spin–orbit coupling produce effects of similar magnitudes. For clarity, in this figure, the effects of the magnetic field have been greatly exaggerated. In order to relate the energy level sequence shown in Fig. 9.2 to experiment, a value for the average magnetic moment per molecule χ_M is needed (see Section 9.2). Now, χ_M is

$$\chi_M = \frac{\sum_{\text{all molecules}} (\text{magnetic moment of a molecule}) \times (\text{number of molecules with this moment})}{(\text{total number of molecules})}$$

There is a Boltzmann distribution of molecules over the levels shown on the right-hand side of Fig. 9.2, so that the relative number of molecules occupying a level with energy E is $\exp(E/kT)$, a quantity which can be used in the expression above provided that we have explicit expressions for the energy levels—and Appendix 10 provides them. The Zeeman part of the calculation provides the value of the magnetic moment for the molecules in a particular level. Having thus obtained a complete expression for χ_M, this can be related to the quantity usually discussed, the Bohr magneton number μ_{eff} because, as was shown in Section 9.2 (eqns 9.4 and 9.5)

$$\mu_{eff}^2 = \frac{3kT\chi_M}{N_A\beta^2} \tag{9.6}$$

Rather than work with the rather unwieldy equations resulting from the expressions given in Appendix 10 we shall simplify. We ignore the tetragonal

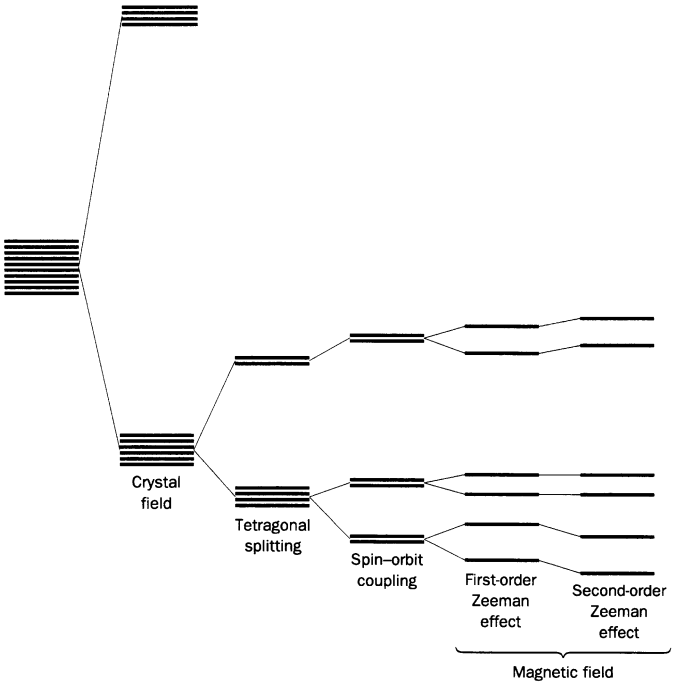

Fig. 9.2 Schematic energy level diagram illustrating the various splittings determining the ground state derived from a t_{2g}^1 configuration.

distortion. With this step we obtain the Kotani model, in which just the effects of spin–orbit coupling and the magnetic field on a t_{2g}^1 configuration are considered. We thus obtain an important expression, derived in reasonable detail in Appendix 10:

$$\mu_{\text{eff}}^2 = \frac{\dfrac{3\zeta}{kT} - 8\exp\left(\dfrac{-3\zeta}{2kT}\right) + 8}{\dfrac{\zeta}{kT}\left[\exp\left(\dfrac{-3\zeta}{2kT}\right) + 2\right]}$$

or, by putting $\zeta/kT = x$ (a number) the equation simplifies to

$$\mu_{\text{eff}}^2 = \frac{(3x - 8)\exp\left(\dfrac{-3x}{2}\right) + 8}{x\left[\exp\left(\dfrac{-3x}{2}\right) + 2\right]}$$

another equation first derived by Kotani.

We can now plot the value of μ_{eff} (given by the positive square root of the above expression) against x, or, more conveniently, against $1/x$, to give a so-called Kotani plot. This has been done in Fig. 9.3. Also on this figure are indicated the values of ζ/kT for some d^1 ions at 300 K, ζ being given the

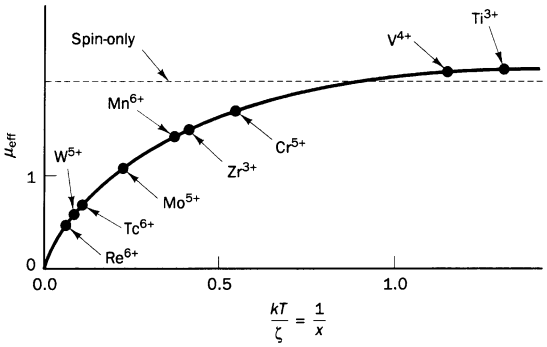

Fig. 9.3 A Kotani plot for the t_{2g}^1 configuration together with 300 K values for some t_{2g}^2 ions. The spin-only formula gives $\mu_{eff} = 1.73$; whereas first row transition metal ions roughly approximate to this value at room temperature, values for second and third row ions can be very different.

free-ion value. It is seen that μ_{eff} is almost independent of temperature at high enough temperatures (the larger ζ, the higher the temperature needed); room temperature measurements on first row transition metal ions give, essentially, their 'plateau' values. It is under these limiting conditions that simple formulae such as

$$\mu_{eff} = \sqrt{n(n+2)}$$

the spin-only formula (which will be derived in the next section), in which n is the number of unpaired electrons, become appropriate. For complexes of the second and third row transition series the spin-only formula is not applicable and magnetic measurements over a temperature range are absolutely essential, even if it is only the number of unpaired electrons which is to be determined. For measurements on such compounds at room temperature, the plateau has not been reached.

For electronic configurations other than the one discussed above, analogous calculations lead to relationships which are roughly similar to that shown in Fig. 9.3. μ_{eff} does not generally drop to zero at 0 K and, down to $\lambda/kT \approx 1.5$ it may increase slightly with decreasing temperature, decreasing as the temperature is lowered further. If the model is not simplified and k (the orbital reduction factor) and t (the factor describing the distortion to a tetragonal field), or related functions, are included in the final energy-level expressions, the temperature dependence of μ_{eff} is less than in the corresponding case in which they are omitted. As an illustration of this, in Fig. 9.4 is shown a comparison between the predicted and experimental results for $[VCl_6]^{2-}$, the cation being the pyridinium ion, $C_5H_5NH^+$. Simple Kotani theory is roughly followed if the spin–orbit coupling constant is reduced to 190 cm^{-1} from the free-ion value of 250 cm^{-1} (Fig. 9.4(a)). Much better agreement is obtained if distortion and covalency are allowed for using the full energy level pattern of Fig. 9.2. This better agreement is shown in Fig. 9.4(b). In that figure, the theoretical curve is that calculated for $k = 0.75$, $\zeta = 150\ cm^{-1}$ and $t = 150\ cm^{-1}$ in the expression given in Appendix 10. The negative sign on t implies that the orbital singlet lies lowest, not the orbital doublet—the distortion is the opposite to that assumed in Appendix 10 and, indeed, earlier in this chapter. The job of fitting a theoretical curve

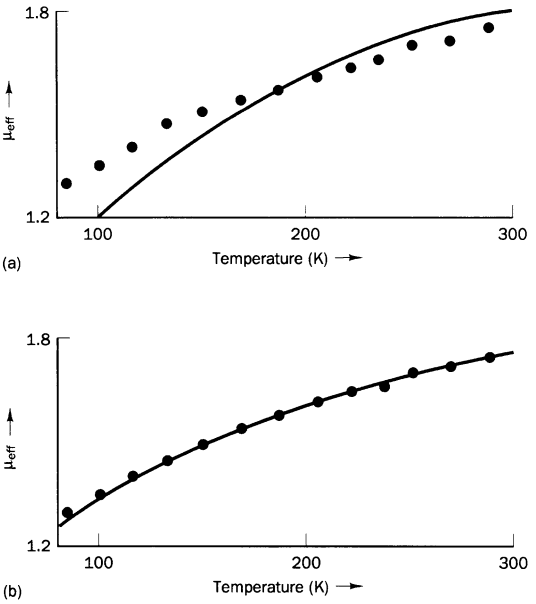

Fig. 9.4 (a) A simple Kotani plot for $[VCl_6]^{2-}$ ($\zeta = 190\ cm^{-1}$). (b) A Kotani plot including best-fit tetragonal distortions and orbital reduction factors. In both cases experimental data are given as dots.

to the experimental results is best done by computer; the need for high experimental accuracy is evident.

This, then, is the algebraic model. What, if anything, is wrong with it? Look again at Fig. 9.4(b), where the best fit between the modified Kotani theory and the experimental data is shown. The lower temperature points seem to show a systematic divergence between experiment and theory. This is not surprising, for as either a qualitative consideration of the effect of decreasing temperature on the population of the levels in Fig. 9.2 or, equivalently, a study of Fig. 9.4(a) (the Kotani plot) shows, the most severe test of the theory is to be expected at the lowest temperatures, for here the average magnetic moment has its greatest temperature dependence. The low-temperature cut-off point in Fig. 9.4 is determined by the boiling point of liquid nitrogen. What if the temperature is taken down to that of liquid helium (3 K), an extension which is now normal. Inevitably, complications set in! These complications can be many-faceted. Small distortions away from true trigonal or tetragonal may become evident, as may long-range magnetic coupling between what would otherwise be regarded as isolated magnetic centres (some examples of this were given at the end of Section 9.1). Fortunately, at such low temperatures it is possible to measure the changes in thermal population of the magnetic-field split levels by another method, that of specific heat measurements. Such additional data are not without additional complications. In particular, the varying thermal population of the multitude of lattice vibrations has to be taken into account. Fortunately, at low temperatures this part of the specific heat of most solids has a T^3

dependence and may usually be allowed for with adequate accuracy. As this example and as the data available in the literature make clear, high temperature magnetic susceptibility data are of limited value—and some would say that 100 K is high—and that much more is revealed at low temperatures. An additional bonus is that at low temperatures it may be possible to use electron paramagnetic (spin) resonance spectroscopy (EPR, discussed in Section 12.6) to study transitions between levels such as those of Fig. 9.2 and so to have independent measures of them. A limited number of ions give room temperature EPR spectra which are well resolved but some which do not are found to give quite sharp lines at low temperatures.

It is here that our circle closes. Such measurements have been made on some Ti^{III} salts and have shown the presence of a major energy contribution which is not present in Fig. 9.2 and is also absent from the associated text and Appendix 10. This contribution arises from a phenomenon that was discussed in Section 8.5, the dynamic Jahn–Teller effect. Throughout our development of the t_{2g}^1 case, we assumed that the molecule under study was rigid. The dynamic Jahn–Teller effect introduces (some, but not all) metal–ligand vibrations into the picture. How important is all this? Well, it has been emphasized earlier that the magnetic properties of a complex are very sensitive to small distortions and therefore to vibrations. The lattice vibrations mentioned above and in Section 9.1 do not distort molecules—in them the molecules move as rigid bodies—and metal–ligand vibrations, also mentioned in Section 9.1, will normally be frozen out at very low temperatures. The dynamic Jahn–Teller effect is much less readily frozen out and so, indeed, it *is* a potential complication. When it is included in the calculation of the energy levels in the t_{2g}^1 case, patterns such as that in Fig. 9.5 are obtained. The difference from Fig. 9.2, although small, is significant. Just as a reasonably complete understanding of the electronic spectra of transition metal complexes requires the inclusion of vibronic (vibrational–electronic) effects so it seems likely that an understanding of magnetism will too. This aspect of the subject is still in its infancy, although it is clear that there are other aspects of the magnetism of coordination compounds in which vibronic effects are implicated (the dynamic Jahn–Teller effect is just one form of vibronic coupling).

The developments outlined in the above paragraph may well help to refute criticisms of that theory of magnetism which has been developed in the last few pages. When data from a large number of complexes were reviewed it was concluded that

1. the theory produces too many ligand field parameters which, in the event, often seem to have no obvious chemical relevance;
2. the models and parameters used for molecules with different geometries seem to bear little relationship with each other; they do not vary with geometry in a way that is obviously sensible;
3. molecules with very low symmetry could not be handled.

Since these criticisms were made the situation has improved, not only because the need to include the dynamic Jahn–Teller effect has been recognized, but also by theoretical developments. Rather than start with an octahedron and distort it, the present tendency is to, theoretically, build up

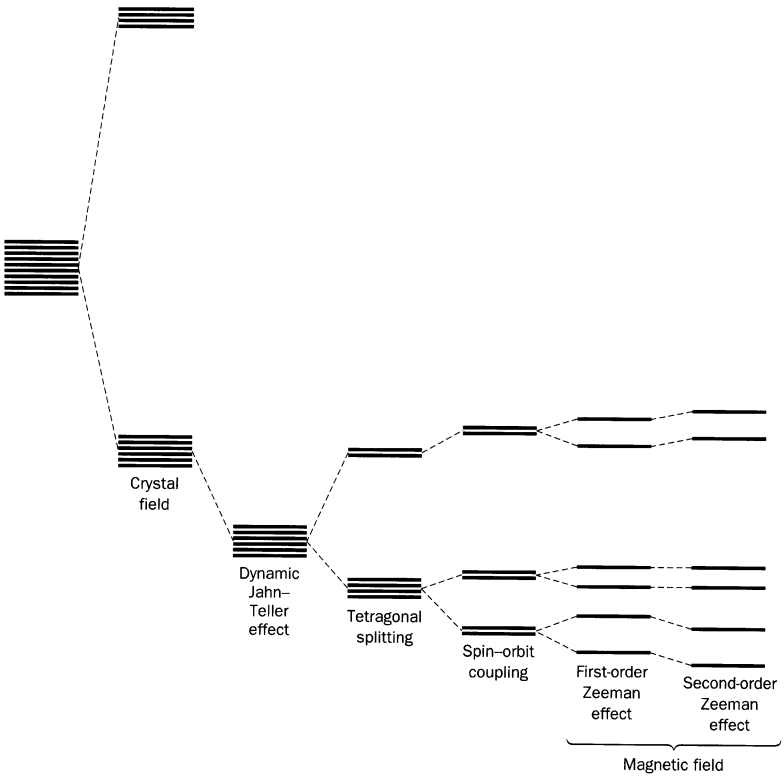

Fig. 9.5 A schematic energy level diagram corresponding to Fig. 9.2 but with inclusion of a dynamic Jahn–Teller effect.

a complex using geometry-sensitive but transferable parameters for each ligand. Surprisingly, an economy of parameters can result. This approach will not be developed here (although the Further Reading at the end of the chapter contains a reference to it) because it tends to be molecule-specific but the general aspects of it will be covered in the next chapter when the angular overlap model is outlined. The reference in the Further Reading at the end of Chapter 10 on modern developments of the angular overlap model provides an entry into the literature on the subject.

9.10 Spin-only equation

The previous section has shown that even if there is an orbital contribution to the magnetic moment it may be reduced by covalency and by distortions. What if we assume that there is no orbital contribution at all—that it is completely quenched? In this section this problem is considered and we will

be led to the spin-only equation mentioned several times earlier in this chapter. The problem will be worked through in some detail to give the reader who has decided not to tackle Appendix 10 some idea of how the calculations are performed.

We are interested in the case in which there are n unpaired electrons, each with spin $\frac{1}{2}$, in an isolated ion which couple to give a resultant, denoted S, where $S = n/2$. The allowed components of S along the direction (z) of a magnetic field, when such a field is applied, are

$$S_z = S,\ (S-1),\ (S-2),\ \ldots,\ (S-(2S-1)),\ (S-2S)$$

That is, the allowed components run from S through to $-S$ and are $(2S+1)$ in number. Their energies in a magnetic field will be proportional to the magnetic field strength and to the magnitude of the z component of S, the value of S_z. So, their energies will be of the form $-2S_z\beta H$, the negative sign indicating that the higher S_z values are stabilized and the 2 being the Landé g factor for the electron—the splittings in a magnetic field are twice as great as one would expect from the magnitude of the spin angular momentum. So, their energies are

$$-2S\beta H,\ -2(S-1)\beta H,\ -2(S-2)\beta H,\ \ldots,\ 2S\beta H$$

The average magnetization per molecule will be given by an expression of the form

$$\frac{\sum(\text{magnetic moment of a molecule}) \times (\text{number with this moment})}{(\text{total number of molecules})}$$

Assuming that in a macroscopic sample there is a Boltzmann distribution of ions over the various S_z levels, we have that the number of ions with moment $2S_z\beta H$ will be $\exp(2S_z\beta H/kT)$. Using this and eqn 9.6 together with eqn 9.1, we obtain

$$\mu_{\text{eff}}^2 = \frac{3kTN_A \sum_{S_z=S}^{-S} 2S_z \times \beta \times \exp\left(\dfrac{2S_z\beta H}{kT}\right)}{N_A\beta^2 \sum_{S_z=S}^{-S} \exp\left(\dfrac{2S_z\beta H}{kT}\right)}$$

Simplifying and expanding the exponentials using the equation $\exp(x) \approx 1 + x$,

$$\mu_{\text{eff}}^2 = \frac{6kT \sum_{S_z=S}^{-S} S_z\left(1 + \dfrac{2S_z\beta H}{kT}\right)}{H\beta \sum_{S_z=S}^{-S} \left(1 + \dfrac{2S_z\beta H}{kT}\right)}$$

This equation contains three standard summations:

$$\sum_{x=a}^{-a} x = 0; \quad \sum_{x=a}^{-a} x^3 = \frac{a}{3}(a+1)(2a+1); \quad \sum_{S_z=S}^{-S} 1 = (2S+1)$$

so,

$$\mu_{\text{eff}}^2 = \frac{6kT}{H\beta} \times \frac{2\beta H}{kT} \times \frac{S}{3} \times (S+1) = 4S(S+1)$$

That is,

$$\mu_{\text{eff}} = 2\sqrt{S(S+1)} = \sqrt{n(n+2)}$$

As we have seen, this relationship holds quite well for the first row transition series. For the second and third row elements it gives totally misleading results because the spin–orbit coupling of these ions is much greater than kT—so that, usually, the plateau of the Kotani plot has not been reached.

9.11 Magnetically non-dilute compounds

When a simple Curie law plot of χ_M against T^{-1} (this pattern was discussed in Section 9.2) does not give a straight line it is often found that a modified form, the Curie–Weiss law, does:

$$\chi_M = \frac{C}{T+\theta}$$

Here, θ is a constant, the Weiss constant, which has the dimensions of temperature, and is measured in degrees. Again, despite its widespread applicability, it is difficult to give a quantum-mechanical interpretation of this relationship. In the limiting cases where this is possible, θ is associated with a breakdown of the Langevin assumption that $B = H$, and values of $\theta \neq 0$ are generally regarded as indicative of magnetic interaction between discrete molecules in condensed phases.

This brings us back to an assumption made at the beginning of this chapter, that we could restrict our discussion to magnetically dilute materials. Magnetically non-dilute materials fall into one of three main classes. These are ferromagnetic, antiferromagnetic and ferrimagnetic—terms that, strictly, apply to extended lattices. In addition we will discuss the phenomenon of ferromagnetic and antiferromagnetic coupling between individual ions, leading to an understanding of the consequences of local magnetic coupling.

In Fig. 9.6 are shown diagrams representing paramagnetism, ferromagnetism, antiferromagnetism and ferrimagnetism, both with and without a (very large!) magnetic field applied. In Fig. 9.7 is shown the temperature behaviour of the magnetism associated with each type. Of the four classes of magnetically non-dilute behaviour shown in Fig. 9.6, that of ferromagnetic behaviour is well known—everyday magnets are made of ferromagnetic materials. As with the other three classes, the individual magnetic centres must be considered together, not separately, the correct building block being the unit cell of the crystalline solid. In ferromagnetic materials, such as metallic iron, the electron spins of each of the atoms couple together to form a resultant unit cell magnetic moment. Iron has a cubic unit cell so let us suppose that the unit cell moment is perpendicular to one of the faces of the unit cell. There are three pairs of such faces and in a perfect crystal of non-magnetized iron there are domains—within each of which there is magnetic alignment between adjacent unit cells—but in the whole crystal there is a random distribution over all of the possible orientations. The process of magnetization brings these moments into alignment and a resultant permanent moment results. These features make ferromagnetic materials quite different from most of those which concern a chemist and

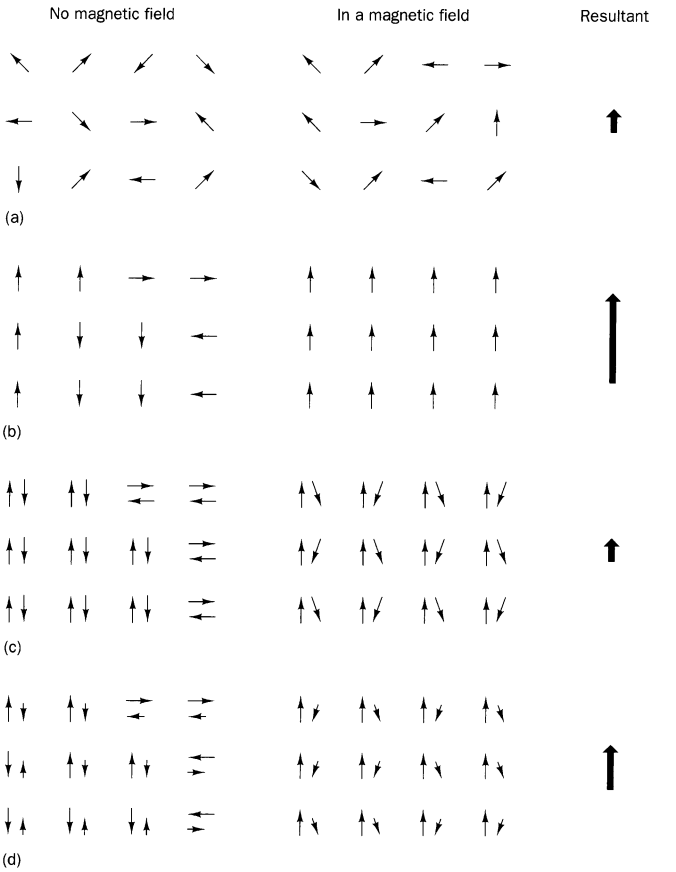

Fig. 9.6 Representations of the most important magnetic phenomena in solids. For simplicity of presentation, the diagrams are more classical than quantum mechanical. (a) Paramagnetism: magnetically dilute materials with zero coupling between adjacent spins. (b) Ferromagnetism: strong coupling leads to a parallel orientation of domains in a strong field. (c) Antiferromagnetism: two, opposed, arrangements which may lead to a domain structure (canted arrangements also occur). At low temperatures the right-hand member of the 'in a magnetic field' pairs settle down to oppose the left hand and the magnetization drops with decrease in temperature. (d) Ferrimagnetism: similar to antiferromagnetism except that the two sets of magnets are of different strength, leading to preservation of magnetism at low temperatures.

we shall not consider them further here, although we shall have something to say about molecular ferromagnetism.

The second—and most important case for the chemist because of its molecular counterpart, to which we shall turn shortly—is that of antiferromagnetism (although we will find that our discussion on this topic takes us to molecular ferromagnetism). In antiferromagnetic materials, transition metal ions are separated by (usually small) ligands, so that many transition metal oxides and halides show antiferromagnetic behaviour. In such compounds, adjacent metal ions couple with their spins antiparallel; there are always equal numbers with the two arrangements so that there is no resultant magnetization in the absence of a magnetic field. As an example of one complicating feature of antiferromagnetism consider the sets of four two-dimensional crystallographic unit cells, as determined by X-ray diffraction,

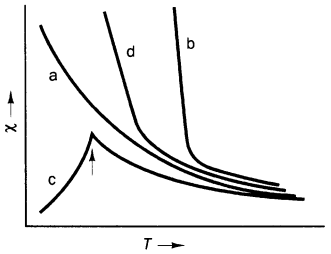

Fig. 9.7 Schematic temperature–susceptibility plots for various types of magnetic behaviour: (a) antiferromagnetism (the arrow indicates the maximum which has sometimes been called the Curie temperature, T_c, or the Néel temperature, T_N); (b) paramagnetism; (c) ferrimagnetism; (d) ferromagnetism. Note that this diagram does not extend to very low temperatures (see Question 9.5, for instance) or high magnetic fields (when saturation effects occur).

shown in Fig. 9.8. X-rays are blind to magnetism[5] and so the magnetic centres are represented by circles in the first diagram (ligands are omitted). We now admit the existence of antiferromagnetic coupling between some pairs of magnetic centres. In the other three sets of cells in this figure are given three possible antiferromagnetic arrangements of spin orientations within the block of four cells. It can be seen that these are all different; the bottom pair of arrangements contain only two *magnetic* unit cells. Compared with the 32 crystallographic point groups and 230 space groups of classical crystallography there are 90 crystallographic magnetic point groups and 1651 magnetic space groups. By using polarized neutrons (neutrons have an intrinsic spin and so behave like tiny bar magnets; in a beam of polarized neutrons these magnets are all essentially parallel), neutron diffraction data are capable of allocating an antiferromagnetic material to its correct magnetic space group. If this is not known, it is not possible to give a complete theoretical discussion of the magnetic properties of an antiferromagnetic material.

Antiferromagnetic materials show a maximum in a plot of χ_M against temperature, at the so-called Néel point—this is shown in Fig. 9.7. Below the Néel point the susceptibility is to some extent field-dependent. These properties provide an indication of the existence, or absence, of antiferromagnetism. Other tests include a comparison of the results of solution and solid-state measurements, where this is possible, and, where it is not, by the technique of the dilution of the magnetic ions in the lattice by their partial substitution with an isomorphous non-magnetic ion. At temperatures sufficiently above the Néel point, antiferromagnetic materials follow a Curie–Weiss law. Even if the Néel point is at too low a temperature to be measured conveniently, the observation that a material follows the Curie–Weiss law usually implies a residual antiferromagnetic coupling.

The third class is that of ferrimagnetic materials. Just as for materials

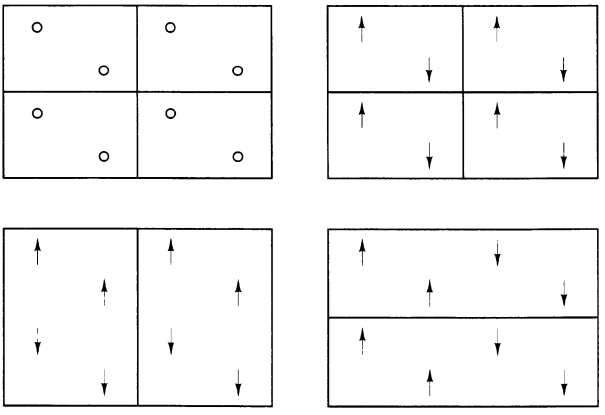

Fig. 9.8 Crystallographic and magnetic unit cells. X-ray diffraction would give for all of these systems the unit cell pattern of the top left-hand diagram. Polarized neutron diffraction would show doubled, magnetic, unit cells for two of them.

[5] This is a marginal overstatement. If the very intense X-ray beam from a synchrotron source is used, weak X-ray magnetic scattering—which is relativistic in origin—can be observed. The effect is rendered more observable by tuning the X-ray energy to coincide with an energy difference in the material under study, when a resonance enhancement occurs.

showing antiferromagnetic behaviour, ferrimagnetic materials have ions on two sets of lattice sites. These have opposed spin arrangements but as they do not cancel each other out there is a resultant permanent moment. The best known example is Fe_3O_4, the black mineral which used to be called magnetic oxide of iron, but which is a complicated case because one site contains (formally) Fe^{II} and Fe^{III} in equal amounts, whilst the other contains only Fe^{III}.

A topic which has gained considerable attention is that of molecular antiferromagnetism (because it potentially leads to the possibility of information storage at the molecular level). This occurs when two transition metal ions both have unpaired electrons and are bonded together, most usually by bridging ligands. In such a case it is common to find that the magnetic properties of the complex are not simply the sum of those of the two individual metal ions. There is a magnetic interaction between them. This situation has already been anticipated at two points in the text. At the end of Section 8.11 it was commented that such magnetic interactions can lead to spectral changes; at the end of Chapter 6 it was recognized that polarized neutron diffraction measurements indicate that the distribution of electrons in a ligand is affected by the unpaired electrons on the metal atom to which it is bonded. The following discussion could be based on the details of Fig. 6.31 but it is simpler to consider a case in which there is bonding between the metal orbital containing the unpaired electron and a ligand pure p orbital. This is shown in Fig. 9.9(a). Because we are interested in a ligand that bridges two transition metal atoms this is the situation pictured in Fig. 9.9(a). Start at the left-hand side of Fig. 9.9(a). The metal ion electron has spin up. Although the ligand p orbital formally contains two electrons, we have seen in Section 6.2.1 that it can nonetheless be involved in bonding with the metal orbital. Such bonding means a pairing between the metal unpaired electron and that of opposite spin in the p orbital. This leaves an election in the p orbital which is of the same spin as that in the left-hand metal d orbital. Pairing between this electron and the metal d electron in the orbital at the right-hand side of the diagram requires that this latter d electron has its spin in the *opposite* direction to that of the d electron in the orbital at the left-hand side of the diagram. That is, the two metal ions are *antiferromagnetically linked* by the ligand. In this example the two metal ions were implicitly taken to be identical. What if they are different? Suppose that one—the left-hand one—has its unpaired electron in an e_g orbital (we assume octahedral symmetry) and the other, the right-hand, has its unpaired electron in a t_{2g}. Starting with the left-hand d orbital, the argument follows that given above until we reach the right-hand d orbital, an orbital which is orthogonal to (that is, has a zero overlap integral with) the ligand p orbital. Unpaired electrons in orthogonal orbitals tend to align themselves with parallel spins (examples of this can be seen by looking back at Fig. 7.10)—this arrangement is exchange-stabilized. In Fig. 9.9(b), therefore, the electron in the right-hand d orbital is of the same spin as that in the left-hand. The two metal ions are *ferromagnetically* linked.

Key to the development of ferromagnetic coupling in the argument above was a step involving the orthogonality of two orbitals. The orthogonality need not be between metal and ligand orbitals. In Fig. 9.9(c) is shown an interaction pathway which includes two p orbitals on the same atom; these

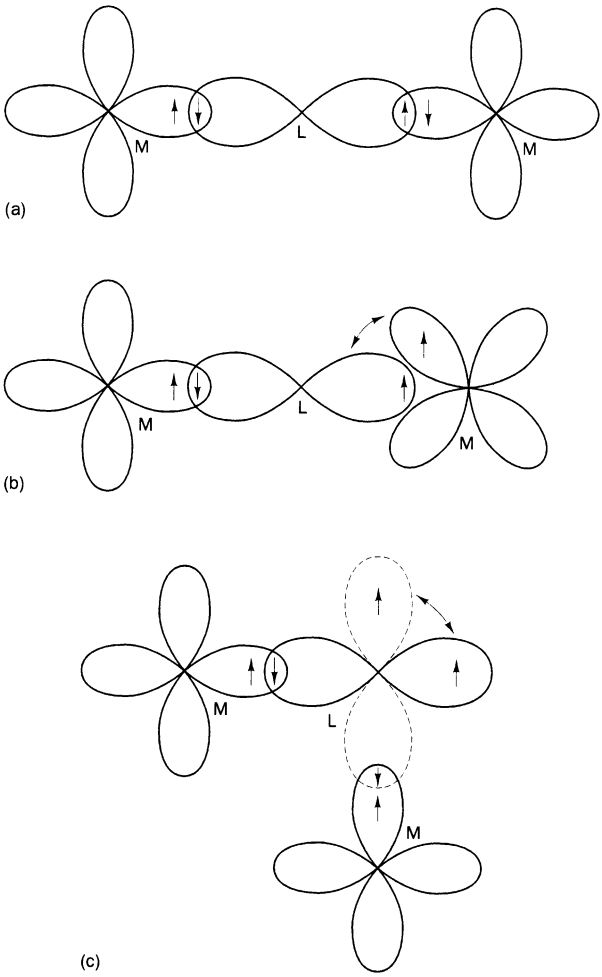

Fig. 9.9 (a) Ligand σ-orbital-mediated antiferromagnetic coupling; (b) and (c) show two ways in which orbital orthogonality can lead to ferromagnetic coupling.

p orbitals, of course, are mutually orthogonal. Again, ferromagnetic coupling results; in Figs. 9.9(b) and 9.9(c) the point at which exchange stabilization leads to parallel spins is indicated by double-headed arrows. It would be sensible for the reader to stop reading at this point and to trace through the pathway of Fig. 9.9(c) and check that a ferromagnetic interaction, indeed, results.

Clearly, by careful choice of metal ions and bridging ligands (which have to be sufficiently rigid to provide rather fixed geometrical relationships between the interacting orbitals) an orthogonal step can be introduced so

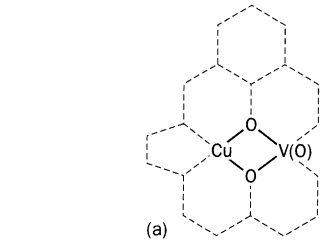

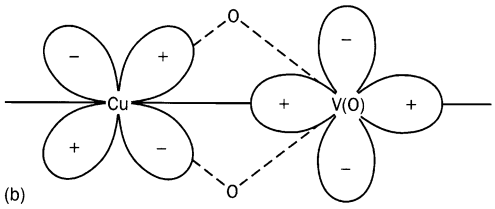

Fig. 9.10 (a) A Cu^{II}–VO complex showing ferromagnetic interaction between the copper and vanadyl ions. The ligand skeleton which holds the two ions together is shown dotted. (b) On the d^9 ion Cu^{2+} an unpaired electron is in an e_g type of orbital; on the d^1 ion VO^{2+} an unpaired electron is in a t_{2g} type of orbital. These orbitals are, respectively, antisymmetric and symmetric with respect to the vertical mirror plane shown as a solid line, and are therefore orthogonal.

that ferromagnetic coupling occurs between two metal atoms, leading them to have parallel spins. An example of such a ligand is shown in Fig. 9.10. Although with cunning choice of ligand and metal ion it is possible to obtain ferromagnetic complexes such as that shown in Fig. 9.10, in most cases the coupling between two linked metal atoms, each with unpaired electrons, will contain at least one antiferromagnetic coupling pathway—a pathway involving non-orthogonal orbitals—and, perhaps, a ferromagnetic coupling through another orbital sequence. In such cases, the antiferromagnetic coupling almost invariably dominates. Lastly, an important word, none the less important for having been left until the end. The discussion of the last few paragraphs hinged on the effects of exchange between electrons on different atoms. Irrespective of whether the outcome is ferromagnetic or antiferromagnetic coupling, the general mechanism involving ligand orbitals to mediate coupling between metal electrons is referred to as *superexchange*.

Finally, although strictly out of place in this chapter, we mention high-temperature superconductors. They are introduced at this point because, as in superexchange, superconductivity involves the properties of electrons on different atoms being correlated with each other. At the time of writing this book the detailed mechanism by which high-temperature superconductivity occurs is not known. The interested reader will find the problem explored in Appendix 11; they should be warned, however, that this appendix is likely to date rather rapidly!

9.12 Spin equilibria

In the final section of this chapter we briefly review some phenomena which, although involving no new concepts, nonetheless lead to some unexpected magnetic results. In Chapter 3 we met two forms of isomerism which have

magnetic implications. Because the splitting of d orbitals is a function of coordination geometry, a change in geometry may well mean a change in the number of unpaired electrons. So, the existence of geometrical isomerism (discussed in Section 3.4.2) may well be magnetically evident (it will be spectrally apparent also). Many examples are provided by Ni^{II} complexes; this ion forms many square planar complexes—which are diamagnetic—which may isomerize to give tetrahedral species. The latter, being d^8, have two unpaired electrons; the reverse isomerization may also occur, of course. This pattern of behaviour is particularly common for Ni^{II} complexes of general formula $[NiP_2X_2]$, where X is a halogen and P is an organophosphine ligand. Typically, the square planar form is red or brown and the tetrahedral green, the Ni^{II} in the latter having a magnetic moment of ca. 3.5 (see Table 9.1).

The second form of isomerism which has magnetic implications is spin isomerism (see Section 3.4.12). This occurs because with the correct choice of ligand (and much effort has been spent on ligand design and variation) the value for Δ, for an octahedral complex can be made to be close to that appropriate to the change-over point from high to low spin complexes in d^4, d^5, d^6 and d^7 systems (see the Tanabe–Sugano diagrams in Appendix 7 for an idea of the magnitude of ligand field required). Most known examples come from the 3d series—Mn^{II}, Mn^{III}, Co^{II}, Co^{III} and, particularly, Fe^{II} and Fe^{III}. Because the two spin states in equilibrium involve different t_{2g}–e_g populations, the metal–ligand bond lengths would be expected to vary between the two spin isomers. X-ray measurements show that the M–L bond lengths tend to be roughly 0.2 Å longer in the high spin form because the e_g orbitals are weakly antibonding and have a higher occupancy in the high spin isomer. Not surprisingly, therefore, the spin equilibria are pressure sensitive, as well as sensitive to the choice of counterion, any solvent of crystallization as well as steric effects originating in the ligands. Many studies have been made of the lifetimes of each of the species in equilibrium. These lifetimes are about 10^{-7} s, but vary by at least one order of magnitude in either direction. Often, the magnetic susceptibility changes on warming a sample are not opposite of those on cooling, this hysteresis indicating some cooperative, perhaps domain, behaviour. Although, magnetically, both spin states are unexceptional, the study of the equilibria between them has been energetically pursued by many workers and has involved the use of almost all of the techniques described in this book (especially those described in Chapter 12), and more.

Further reading

The literature on this subject tends to divide between the old, which provides the best available treatment of the classical (including the classical quantum mechanical), and the recent, which provides an up-dating of the earlier. Older are:

- *Magnetism and Transition Metal Complexes* F. E. Mabbs and D. J. Machin, Chapman & Hall, London, 1973.
- 'The Magnetochemistry of Complex Compounds' B. N. Figgis and J. Lewis, Chapter 6 in *Modern Coordination Chemistry* J. Lewis and R. G. Wilkins (eds.), Interscience, New York, 1960.
- 'The Magnetic Properties of Transition Metal Complexes' B. N. Figgis and J. Lewis, *Prog. Inorg. Chem.* (1964) *6*, 37
- A useful review which also includes an extensive compilation of diamagnetic corrections is 'Magnetochemistry—Advances in Theory and Experimentation' C. J. O'Connor, *Prog. Inorg. Chem.* (1982) *26*, 203
- A still-current view of theory, experiment and problems is

- 'A Local View of Magnetochemistry' M. Gerloch, *Inorg. Prog. Chem.* (1979) *26*, 1.

Problems in the effects of magnetic coupling are reviewed in 'Magnetochemistry: a research proposal' R. L. Carlin, *Coord. Chem. Rev.* (1987) *79*, 215.

An excellent current book is *Molecular Magnetism* O. Kahn, VCH, Weinheim, 1993; a rather different account is 'Organic and Organometallic Molecular Magnetic Materials—Designer Magnets', a very long review by J. S. Miller and A. J. Epstein in *Angew. Chem., Int. Ed.* (1994) *33*, 385.

A detailed account of magnetic phases and phase transitions at low temperatures is 'Magnetic phase transitions at low temperatures' J. E. Rives, *Transition Met. Chem.* (1972) *7*, 1. A more general account is 'Magnetic Symmetry' by W. Opechowski and R. Guccione, Chapter 3 in *Magnetism*, Volume IIA, G. T Rado and H. Suhl (eds.), Academic Press, New York, 1965.

More recent, and concentrating on systems of two transition metal ions, is 'Magnetism of the Heteropolymetallic Systems' O. Kahn, *Struct. Bonding* (1987) *68*, 89.

Spin equilibria are covered in

- 'Dynamics of Spin Equilibria in Metal Complexes' J. K. Beattie, *Adv. Inorg. Chem.* (1988) *32*, 1.
- 'Static and Dynamic Effects in Spin Equilibrium Systems' *Coord. Chem. Rev.* (1988) *86*, 245.

Questions

9.1. Show that the metal d orbital and the ligand σ orbitals that contain unpaired spin density in Fig. 6.31 are orthogonal to each other. (Hint: consider their symmetries.)

9.2. Show that the interactions shown in Fig. 9.9(c) lead to a ferromagnetic (parallel spin) coupling of the two metal ions.

9.3. If one step involving orthogonal interactions leads to a ferromagnetic interaction, then two such steps should lead to an antiferromagnetic. Check this conclusion by replacing one of the d orbitals shown in Fig. 9.9(c) by a t_{2g} d orbital and tracing through the coupling pathway.

9.4. Figure 9.8 does not exhaust the possible two-dimensional antiferromagnetic arrangements of two magnetic ions; three more are shown in Fig. 9.11. However, unit cells similar to those of Fig. 9.8 are not given. Insert them. To complete this task for the third diagram will require the recognition of a feature not discussed in the text.

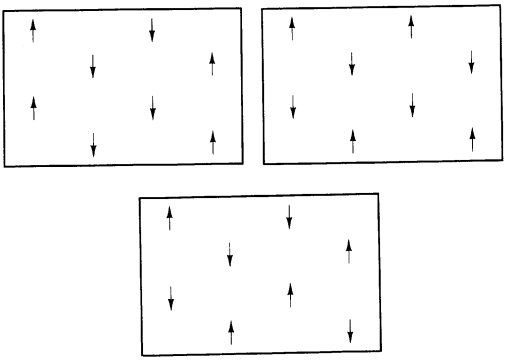

Fig. 9.11 Question 9.4.

9.5. In Fig. 9.9 and the associated discussion within the text, the ligand orbital involved in superexchange was a σ orbital. Ligand π orbitals may also be involved. Figure 9.12 is the ligand π orbital equivalent of Fig. 9.9(a). Give an account of Fig. 9.12 which parallels that given in the text for Fig. 9.9(a).

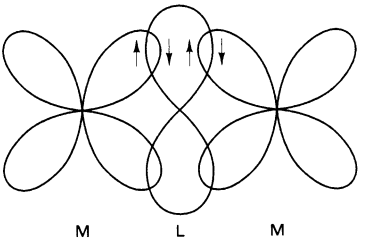

Fig. 9.12 Question 9.5.

9.6. There is a, perhaps, unexpected result contained in Fig. 9.4. At 0 K a system with a single unpaired electron is predicted to be non-magnetic. Give a qualitative explanation for this behaviour (remember—there are two sources of magnetism, orbital and spin).